2400 *Organometallics* **2001,** *20,* 2400−2404

Ru-σ-butadiynyl Complexes of the Tetraanilinopyridinatodiruthenium Core: Formation of a Bis-adduct

Guolin Xu and Tong Ren*

Department of Chemistry and Center for Supramolecular Science, University of Miami, Coral Gables, Florida 33124

Received December 13, 2000

The stoichiometric reaction between $Ru_2(ap)_4Cl$ (*ap* = 2-anilinopyridinate) and LiC≡CC≡CSiMe$_3$ yielded $Ru_2(ap)_4$(C≡CC≡CSiMe$_3$) (**1**) as the only product. A similar reaction utilizing a 5-fold excess of LiC≡CC≡CSiMe$_3$ resulted in a mixture of **1** and the bis-alkynyl adduct *trans*-$Ru_2(ap)_4$(C≡CC≡CSiMe$_3$)$_2$ (**2**), and the ratio of two products depends on workup procedures. X-ray diffraction studies of **1** and **2** revealed that the bridging *ap* ligands are in the (4,0) polar arrangement and the Ru−Ru vector and butadiynyl backbone are approximately collinear. Both compounds **1** and **2** are rich in redox chemistry: two reversible one-electron couples were observed for the former and three for the latter from the cyclic voltammetry study.

Introduction

We are interested in linear rigid rods based on oligometallayne **A** (Scheme 1). With an extensive π-conjugation along the backbone, these rods may be developed as *conducting* molecular wires.[1−3] The existence of significant electronic delocalization along the backbone has been demonstrated in recent years for type **A** rods (n = 1) with [M] as CpFe(P−P),[4] CpRe(P)(NO),[5] CpRu(P)$_2$,[6] and Mn(P−P)$_2$I[7] (P and P−P are mono- and bidentate phosphines, respectively). However, the oligomeric form of **A** ($n > 1$) based on the above-mentioned termini is currently unknown, which may be attributed to the absence of a coordination site *trans* to the existing carbyne ligand (except [M] = Mn(P−P)$_2$I) that is required for an extended linear rod.[3]

Scheme 1. (*a*) Oligometallayne Rod; *m*, *n* = Integers; (b) Rod with [Ru$_2$(*ap*)$_4$] Terminus, *m* = 1 and 2

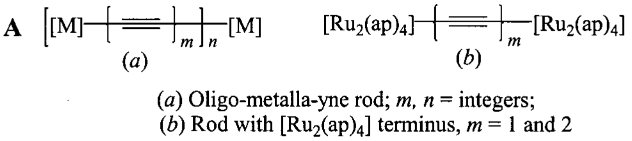

Recently, we reported a series of type **A** rigid rods with bimetallic termini ((*b*) in Scheme 1),[8] where substantial electronic delocalization between two [Ru$_2$(*ap*)$_4$] termini across the (C≡C)$_m$ bridge has been demonstrated through both electrochemical and spectroscopic studies. In principle, these rods could be extended further since each [Ru$_2$(*ap*)$_4$] terminus has an open axial site *trans* to the existing carbyne chain. Hence, the hope of achieving a type **A** rod with $n > 1$ is largely hinged upon the realization of bis-alkynyl adducts of the [Ru$_2$(*ap*)$_4$] core. However, early investigation of reactions between [Ru$_2$(*ap*)$_4$]Cl and various alkynyl ligands (M′C≡CR, M′ = Li and SnMe$_3$, R = SiMe$_3$, Ph, and CH$_2$OCH$_3$) led to the isolation of [Ru$_2$(*ap*)$_4$](C≡CR) only.[9−11] While metal complexes bearing one polyynyl ligand have become commonplace in recent years, bis-polyynyl complexes, especially those with a *trans*-arrangement, remain rare.[12−16] To our knowledge, there exist only three structurally established examples of *trans*-polyynyl compounds, i.e., *trans*-Ru(CO)$_2$(PEt$_3$)$_2$-[(C≡C)$_2$R]$_2$ (R = H and SiMe$_3$) by Carty et al.[14] and *trans*-Ru$_2$(D*m*AniF)$_4$[(C≡C)$_2$SiMe$_3$]$_2$ by us (D*m*AniF is di(*m*-methoxyphenyl)formamidinate).[16] Further characterization of the bis-polyynyl adducts on the [Ru$_2$(ap)$_4$] core will certainly enrich the understanding of metal-polyynyl compounds. We report herein that by treating Ru$_2$(*ap*)$_4$Cl with lithium butadiynyl, both the mono- and bis-adducts (**1** and **2** in Scheme 2, respectively) can be

---

* Corresponding author. Tel: (305) 284-6617. Fax: (305) 284-1880. E-mail: tren@miami.edu.

(1) Paul, F.; Lapinte, C. *Coord. Chem. Rev.* **1998**, *178−180*, 431.

(2) Martin, R. E.; Diederich, F. *Angew. Chem., Int. Ed. Engl.* **1999**, *38*, 1350.

(3) Schwab, P. F. H.; Levin, M. D.; Michl, J. *Chem. Rev.* **1999**, *99*, 1863.

(4) Le Narvor, N.; Toupet, L.; Lapinte, C. *J. Am. Chem. Soc.* **1995**, *117* (7), 7129.

(5) Brady, M.; Weng, W.; Zou, Y.; Seyler, J. W.; Amoroso, A. J.; Arif, A. M.; Bohme, M.; Frenking, G.; Gladysz, J. A. *J. Am. Chem. Soc.* **1997**, *119*, 775.

(6) Bruce, M. I.; Low, P. J.; Costuas, K.; Halet, J.-F.; Best, S. P.; Heath, G. A. *J. Am. Chem. Soc.* **2000**, *122*, 1949.

(7) Kheradmandan, S.; Heinze, K.; Schmalle, H. W.; Berke, H. *Angew. Chem., Int. Ed.* **1999**, *38*, 2270.

(8) Ren, T.; Zou, G.; Alvarez, J. *Chem. Commun.* **2000**, 1197.

(9) Chakravarty, A. R.; Cotton, F. A. *Inorg. Chim. Acta* **1986**, *113*, 19.

(10) Zou, G.; Alvarez, J. C.; Ren, T. *J. Organomet. Chem.* **2000**, *596*, 152.

(11) Cotton, F. A.; Stiriba, S. E.; Yokochi, A. *J. Organomet. Chem.* **2000**, *595*, 300.

(12) Sonogashira, K.; Kataoka, S.; Takahashi, S.; Hagihara, N. *J. Organomet. Chem.* **1978**, *160*, 319.

(13) Sonogashira, K.; Ohga, K.; Takahashi, S.; Hagihara, N. *J. Organomet. Chem.* **1980**, *188*, 237.

(14) Sun, Y.; Taylor, N. J.; Carty, A. J. *Organometallics* **1992**, *11*, 4293.

(15) Touchard, D.; Pirio, N.; Troupet, L.; Fettouhi, M.; Ouahab, L.; Dixneuf, P. H. *Organometallics* **1995**, *14*, 5263.

(16) Xu, G.; Ren, T. *Inorg. Chem.* **2001**, *40*, in press.

10.1021/om001064l CCC: $20.00

Scheme 2. Structures of Mono- and Bis-butadiynyl Adducts of $[Ru_2(ap)_4]$ Core

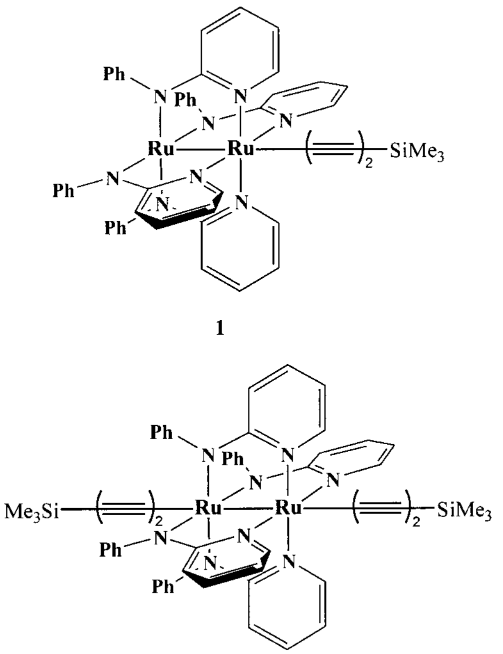

obtained. Also reported are the crystallographic and electrochemical characterizations of these new compounds.

Results and Discussion

Similar to our earlier synthesis of $Ru_2(ap)_4(C{\equiv}CSiMe_3)$,[10] the stoichiometric reaction between $Ru_2(ap)_4Cl$ and $LiC{\equiv}CC{\equiv}CSiMe_3$ produced the mono-adduct $Ru_2(ap)_4(C{\equiv}CC{\equiv}CSiMe_3)$ (**1**) in excellent yield. When a 5-fold excess of $LiC{\equiv}CC{\equiv}CSiMe_3$ is used, the bis-adduct *trans*-$Ru_2(ap)_4(C{\equiv}CC{\equiv}CSiMe_3)_2$ (**2**) is isolated in addition to **1**. Yields of compounds **1** and **2** depend on the workup procedures. The mono-adduct **1** is dominant when solvent is removed from the reaction mixture *in vacuo* prior to the exposure to air. In contrast, the bis-adduct **2** is the major product when the mixture is stirred in air prior to solvent removal. While the dependence of mono-/bis-ratio upon the workup procedure is similar to that reported for the reaction between chlorotetrakis(diarylformamidinate)-diruthenium(II,III) and excess $LiC{\equiv}CPh$,[17−19] the combined yield of **1** and **2** based on Ru is much higher (ca. 90% from both workups), indicating the absence of side-reactions.

Successful isolation of **2** prompted us to examine the possibility of the formation of $Ru_2(ap)_4(C{\equiv}CSiMe_3)_2$ via treating $Ru_2(ap)_4Cl$ with excess $LiC{\equiv}CSiMe_3$. However, $Ru_2(ap)_4(C{\equiv}CSiMe_3)$ remains as the sole product with up to a 10-fold excess of $LiC{\equiv}CSiMe_3$. Obviously, the steric repulsion between the phenyl groups of the *ap* ligand and the $SiMe_3$ group prohibits the binding of $C{\equiv}CSiMe_3$ at the second axial site. The steric repulsion becomes negligible with the longer polyynyl, $C{\equiv}CC{\equiv}CSiMe_3$, as the incoming ligand.

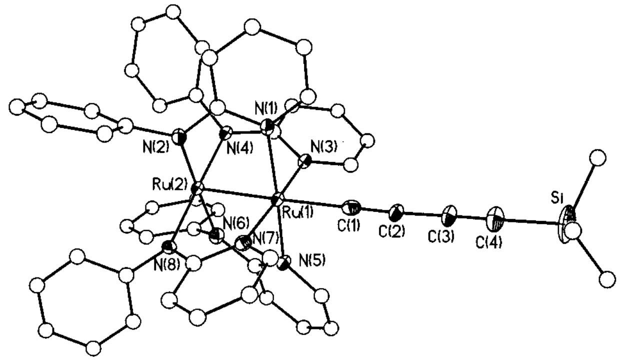

Figure 1. ORTEP plot of molecule **1** at 20% probability level.

The molecular structure of compound **1** is shown in Figure 1, and the coordination geometry around the Ru_2 core is quite similar to that of $Ru_2(ap)_4(C{\equiv}CSiMe_3)$.[10] The 2-anilinopyridinates coordinate in the so-called (4,0) polar arrangement, where all the pyridine nitrogens bond to the Ru-center bearing the axial butadiynyl ligand and all the anilino nitrogens to the other Ru-center. The Ru−Ru (2.330(1) Å) and $Ru{-}C_\alpha$ (2.075(9) Å) bond distances are nearly identical to these of $Ru_2(ap)_4(C{\equiv}CSiMe_3)$ (2.316(1) and 2.077(4) Å, respectively). The average Ru(II)−N and Ru(III)−N bond lengths are 2.047(6) and 2.108(7) Å for **1** and 2.046(2) and 2.095(5) Å for $Ru_2(ap)_4(C{\equiv}CSiMe_3)$. The C−C bond lengths of the butadiynyl ligand generally conform to the formalism of alternating C−C single and triple bonds. Although each of the bond angles along the $Ru{-}C{\equiv}C{-}C{\equiv}C{-}Si$ linkage deviates from 180° by no more than 3°, the deviations are additive and lead to a smooth curvature of the $Ru{-}C{\equiv}C{-}C{\equiv}C{-}Si$ backbone. Besides the structural similarity, molecule **1** is also isoelectronic to $Ru_2(ap)_4(C{\equiv}CSiMe_3)$,[10] as evidenced by a $S = 3/2$ ground state (effective magnetic moment at room temperature is 3.85 μ_B).[20]

Compound **2** displays a sharp and well-resolved ^1H NMR spectrum, which contains two equally intense signals attributed to the $SiMe_3$ groups. The NMR spectrum verifies that compound **2** is diamagnetic and retains the polar (4,0) arrangement of bridging *ap* ligands. The retention of such a polar arrangement is not surprising since the synthesis was conducted at room temperature. To determine whether compound **2** can undergo thermal rearrangement to the less polar *trans*/*cis*-(2,2) configuration, a THF solution of **2** was heated. No change was detected when heating around 60 °C, but prolonged refluxing led to the complete conversion of **2** to strongly polar, unidentified product(s).

The (4,0) arrangement of the *ap* bridging ligands and other fine structural details of compound **2** were revealed by the X-ray structure determination, and a structural perspective is presented in Figure 2. The selected bond lengths and angles for compounds **1** and **2** are collected in Table 1. The most significant structural change from the mono- (**1**) to bis-adduct (**2**) is the

---

(17) Bear, J. L.; Han, B.; Huang, S.; Kadish, K. M. *Inorg. Chem.* **1996**, *35*, 3012.

(18) Lin, C.; Ren, T.; Valente, E. J.; Zubkowski, J. D. *J. Chem. Soc., Dalton Trans.* **1998**, 571.

(19) Lin, C.; Ren, T.; Valente, E. J.; Zubkowski, J. D. *J. Organomet. Chem.* **1999**, *579*, 114.

(20) Cotton, F. A.; Walton, R. A. *Multiple Bonds between Metal Atoms*; Oxford University Press: Oxford, 1993.

Table 1. Selected Bond Lengths (Å) and Angles (deg) for Compounds $1\cdot C_4H_8O_2$ and 2

$1\cdot C_4H_8O_2$		2			
Ru(1)−Ru(2)	2.3303(9)	Ru(1)−Ru(2)	2.4717(11)	Ru(2)−N(8)	1.948(7)
Ru(1)−C(1)	2.075(9)	Ru(1)−C(1)	1.938(11)	C(1)−C(2)	1.216(13)
Ru(1)−N(1)	2.122(6)	Ru(2)−C(8)	1.956(9)	C(2)−C(3)	1.394(15)
Ru(1)−N(3)	2.098(6)	Ru(1)−N(1)	2.045(8)	C(3)−C(4)	1.208(14)
Ru(1)−N(5)	2.096(7)	Ru(1)−N(3)	1.971(8)	Si(1)−C(4)	1.819(12)
Ru(1)−N(7)	2.115(6)	Ru(1)−N(5)	2.031(8)	C(8)−C(9)	1.228(13)
Ru(2)−N(2)	2.031(7)	Ru(1)−N(7)	2.124(8)	C(9)−C(10)	1.386(16)
Ru(2)−N(4)	2.051(6)	Ru(2)−N(2)	1.995(8)	C(10)−C(11)	1.227(15)
Ru(2)−N(6)	2.052(7)	Ru(2)−N(4)	2.186(7)	Si(2)−C(11)	1.803(14)
Ru(2)−N(8)	2.055(6)	Ru(2)−N(6)	1.998(8)		
C(1)−C(2)	1.207(11)				
C(2)−C(3)	1.406(11)				
C(3)−C(4)	1.208(11)				
Si−C(4)	1.832(10)				
C(1)−Ru(1)−Ru(2)	178.3(3)	C(1)−Ru(1)−Ru(2)	162.9(3)	N(8)−Ru(2)−Ru(1)	94.0(2)
N(1)−Ru(1)−Ru(2)	86.77(16)	C(8)−Ru(2)−Ru(1)	164.0(3)	C(2)−C(1)−Ru(1)	178.5(9)
N(3)−Ru(1)−Ru(2)	88.27(16)	N(1)−Ru(1)−Ru(2)	86.3(2)	C(1)−C(2)−C(3)	177.7(11)
N(5)−Ru(1)−Ru(2)	88.24(17)	N(3)−Ru(1)−Ru(2)	97.2(2)	C(4)−C(3)−C(2)	178.3(12)
N(7)−Ru(1)−Ru(2)	87.80(17)	N(5)−Ru(1)−Ru(2)	87.6(2)	C(3)−C(4)−Si(1)	170.3(11)
N(2)−Ru(2)−Ru(1)	89.90(17)	N(7)−Ru(1)−Ru(2)	77.66(19)	C(9)−C(8)−Ru(2)	175.3(8)
N(4)−Ru(2)−Ru(1)	88.78(17)	N(2)−Ru(2)−Ru(1)	87.2(2)	C(8)−C(9)−C(10)	172.4(11)
N(6)−Ru(2)−Ru(1)	89.11(17)	N(4)−Ru(2)−Ru(1)	76.1(2)	C(11)−C(10)−C(9)	176.2(13)
N(8)−Ru(2)−Ru(1)	89.62(17)	N(6)−Ru(2)−Ru(1)	86.4(2)	C(10)−C(11)−Si(2)	174.7(13)
C(2)−C(1)−Ru(1)	179.5(8)				
C(1)−C(2)−C(3)	177.1(9)				
C(4)−C(3)−C(2)	178.4(11)				
C(3)−C(4)−Si	178.5(10)				
N(1)−Ru(1)−Ru(2)−N(2)	19.8(2)	N(1)−Ru(1)−Ru(2)−N(2)	18.4(3)		
N(3)−Ru(1)−Ru(2)−N(4)	19.4(2)	N(3)−Ru(1)−Ru(2)−N(4)	22.4(3)		
N(5)−Ru(1)−Ru(2)−N(6)	16.2(2)	N(5)−Ru(1)−Ru(2)−N(6)	15.5(3)		
N(7)−Ru(1)−Ru(2)−N(8)	17.0(2)	N(7)−Ru(1)−Ru(2)−N(8)	24.7(3)		

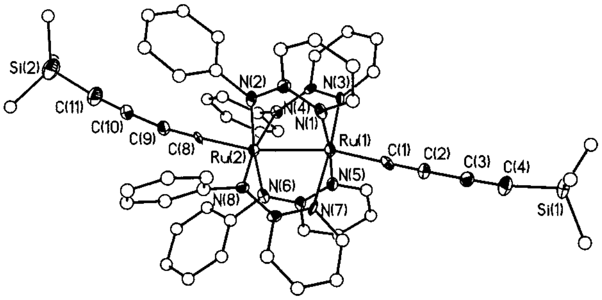

Figure 2. ORTEP plot of molecule **2** at 20% probability level.

elongation of the Ru−Ru bond from 2.330(1) to 2.472(1) Å, which can be attributed to both the increase in the formal oxidation state from (II,III) to (III,III) and the depletion of Ru−Ru σ-bonding electron density via the formation of a new Ru−C bond. Similar structural changes from mono- to bis-adducts were observed in our earlier studies of diruthenium complexes bearing phenylacetylide axial ligands.[18,19] The axial Ru−C σ-bonds in **2** are shortened by at least 0.12 Å from that of **1**, reflecting both the enhancement of Ru−C bonding (major) and the reduction in the Ru covalent radius (minor). Furthermore, the coordination geometry of the bridging *ap* ligands is severely distorted from a typical paddle-wheel motif. Of four Ru(1)−N bonds formed with pyridine nitrogen, the Ru(1)−N(3) bond length is much shorter than the average (2.043(8) Å), while the Ru(1)−N(7) bond (*trans* to N(3)) is significantly elongated. For the anilino nitrogens, the Ru(2)−N(4) bond is the longest, and the bond *trans* to it (Ru(2)−N(8)) the shortest. Large variation among Ru−Ru−N angles can also be observed from the data in Table 1. As elaborated for the case of Ru_2(diarylformamidinate)$_4$(C≡CPh)$_2$,[18] the observed structural distortion is attributed to a second-order Jahn−Teller effect, which is induced by the formation of strong Ru−C σ-bonds.

A comparison of **2** with both *trans*-$Ru(CO)_2(PEt_3)_2$-$[(C{\equiv}C)_2SiMe_3]_2$ (**3**)[14] and *trans*-Ru_2(D*m*AniF)$_4$-$[(C{\equiv}C)_2SiMe_3]_2$ (**4**)[16] provides information on the effect of the transition metal environment on the geometry of butadiynyl ligands. In molecule **2**, one of two butadiynyl ligands (**a**) bonds to the Ru-center supported by the pyridino-nitrogen donors, while the other bonds to the Ru-center supported by the anilino-nitrogen donors (**b**). Despite the difference in the chemical environments, two butadiynyl ligands exhibited similar bond lengths and angles. As shown by the relevant interatomic parameters listed in Table 2, the Ru−C_α bond length in the diruthenium(III) compounds (**2** and **4**) is at least 0.10 Å shorter than that of the mononuclear ruthenium(II) compounds (**3**), indicating an enhancement of Ru−C bonding due to the increase in the formal oxidation state. However, no *statistically* significant variation in the bond lengths and angles of butadiynyls among compounds **2**−**4** is observed. The insensitivity of the $C_\alpha{\equiv}C_\beta$ distances toward the formal oxidation state of the ruthenium center implies the absence of π-back-bonding interaction.

An essential feature of the building blocks for *molecular wire* is the ability to function as an electron reservoir[3] and undergo both oxidation and reduction reversibly. This is clearly the case for both molecules **1** and **2**, as revealed in their cyclic voltammograms (Figure 3).

Prior studies of Ru_2(*ap*)$_4$(C≡CR),[10] Ru_2(form)$_4$-(C≡CPh),[19] and Ru_2(form)$_4$(C≡CPh)$_2$[18] revealed three possible oxidation couples for these diruthenium species as assigned below according to the formal oxidation state of the Ru centers:

$$\mathrm{Ru_2(III,IV)} \underset{\mathbf{A}}{\overset{+\,e^-}{\rightleftharpoons}} \mathrm{Ru_2(III,III)} \underset{\mathbf{B}}{\overset{+\,e^-}{\rightleftharpoons}} \mathrm{Ru_2(III,II)} \underset{\mathbf{C}}{\overset{+\,e^-}{\rightleftharpoons}} \mathrm{Ru_2(II,II)}$$

Table 2. Interatomic Parameters of the Coordinated Butadiynyl Ligands

	trans-$Ru_2(ap)_4(C{\equiv}CC{\equiv}CSiMe_3)_2$		*trans*-$Ru(CO)_2(PEt_3)_2$ $(C{\equiv}CC{\equiv}CSiMe_3)_2$ (**3a**)[14]	*trans*-$Ru_2(DmAniF)_4$ $(C{\equiv}CC{\equiv}CSiMe_3)_2$ (**4**)[16]
	a	**b**		
$Ru-C_\alpha$	1.938(11)	1.956(9)	2.057(2)	1.947(2)
$C_\alpha-C_\beta$	1.216(13)	1.228(13)	1.226(2)	1.206(3)
$C_\beta-C_\gamma$	1.394(15)	1.386(16)	1.370(2)	1.371(4)
$C_\gamma-C_\delta$	1.208(14)	1.227(15)	1.209(2)	1.196(4)
$Ru-C_\alpha-C_\beta$	178.5(9)	175.3(8)	176.5(2)	175.2(2)
$C_\alpha-C_\beta-C_\gamma$	177.7(11)	172.4(11)	178.9(2)	177.3(3)
$C_\beta-C_\gamma-C_\delta$	178.3(12)	176.2(13)	179.8(3)	179.2(5)

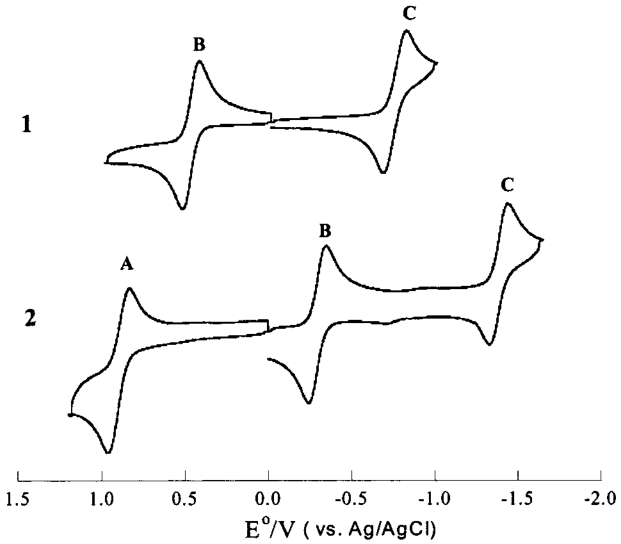

Figure 3. Cyclic voltammograms of compounds **1** and **2** recorded in a 0.20 M THF solution of Bu_4NPF_6 at a scan rate of 0.10 V/s.

For the mono-adduct **1**, a Ru_2(II,III) compound, both an oxidation (**B**, 0.48 V) and a reduction (**C**, −0.74 V) couple were observed, and both are quasi-reversible based on ΔE_p values and $i_{backward}/i_{forward}$ ratios. Our earlier study of compounds bearing axial ethynyl ligand (C≡CR with R = H, $SiMe_3$, Ph, CH_2OCH_3) revealed that the potential for couple **B** occurs around 0.20 V and the potential for couple **C** around −1.02 V.[10] An anodic shift of 0.28 V in electrode potentials from the compounds bearing an ethynyl ligand to **1** is attributed to the reduced nucleophilicity of the butadiynyl ligand.

For the bis-adduct **2**, a Ru_2(III,III) compound, three quasi-reversible couples are observed at the potentials 0.90 (**A**), −0.29 (**B**), and −1.38 V (**C**). In a comparison of the potentials for the (III,III)/(III,II) and (III,II)/(II,II) couples, a shift of ca. −0.70 V from **1** to **2** is noted. This shift reflects an increased stabilization of the higher oxidation state of the Ru_2-core upon addition of a σ-bonded butadiynyl. A similar trend is also observed in the phenylethynyl adducts.[18,19]

In conclusion, we have demonstrated that *trans*-$\{Ru_2(ap)_4[(CC)_mR]_2\}$ compounds are attainable by using butadiynyl ligand ($m = 2$). Currently, we are exploring both the synthesis of analogous compounds with $m > 2$ and the utility of compounds **1** and **2** as the building blocks of conjugated metallaynes.

Experimental Section

n-BuLi and 2-anilinopyridine were purchased from Aldrich, 1,4-bistrimethylsilyl-1,3-butadiyne was from Lancaster, and silica gel was from Merck. $Ru_2(ap)_4Cl$ was prepared as previously described.[10] THF and hexanes were distilled over Na/benzophenone under an N_2 atmosphere prior to use. ^1H and ^{13}C NMR spectra were recorded on a Bruker AVANCE300 NMR spectrometer, with chemical shifts (δ) referenced to the residual $CHCl_3$ and the solvent $CDCl_3$, respectively. Infrared spectra were recorded on a Perkin-Elmer 2000 FT-IR spectrometer using KBr disks. UV−vis spectra were obtained with a Perkin-Elmer Lambda-900 UV−vis spectrophotometer. Magnetic susceptibility was measured at 293 K with a Johnson Matthey Mark-I magnetic susceptibility balance. Elemental analysis was performed by Atlantic Microlab, Norcross, GA. Cyclic voltammograms were recorded in 0.2 M $(n\text{-Bu})_4NPF_6$ solution (THF, N_2-degassed) on a CHI620A voltammetric analyzer with a glassy carbon working electrode (diameter = 2 mm), a Pt-wire auxiliary electrode, and a Ag/AgCl reference electrode. The concentration of diruthenium species is always 1.0 mM. The ferrocenium/ferrocene couple was observed at 0.582 V (vs Ag/AgCl) at the experimental conditions.

Stoichiometric Reaction between $Ru_2(ap)_4Cl$ and LiC≡CC≡CSiMe$_3$. To a 20 mL THF solution containing 0.4 mmol of $Me_3SiC{\equiv}CC{\equiv}CSiMe_3$ was added 0.25 mL of BuLi (1.6 M in hexanes) at −80 °C. The mixture was slowly warmed to room temperature and stirred for another hour to yield an off-white suspension. Half of the suspension was transferred to a flask containing a THF solution (20 mL) of $Ru_2(ap)_4Cl$ (0.184 g, 0.20 mmol). The solution color changed from dark green to brown immediately, and the reaction mixture was stirred for an hour. Removal of the solvents in vacuo yielded a brown residue, which was rinsed with copious amounts of warm methanol and filtered. A brownish-green solid was obtained after drying in a vacuum and identified as the analytically pure $Ru_2(ap)_4(C{\equiv}CC{\equiv}CSiMe_3)$ (**1**). Yield: 160 mg (81%).

Data for 1: R_f 0.76 (Et_3N/ethyl acetate/hexanes, 1/1/10, v/v). MS−FAB (*m/e*, based on ^{101}Ru): 1000 [M^+]. Anal. for $C_{55}H_{53}N_8O_2SiRu_2$ (**1**·EtOAc), found (calcd): C, 60.7 (60.0); H, 4.91 (4.99); N, 10.3 (10.2). UV−vis, λ_{max} (nm, ϵ (M^{-1} cm^{-1})): 763(5400), 492(7290). IR, ν(C≡C)/cm^{-1}: 2109(w), 2143(w). Electrochemical, $E_{1/2}$/V, ΔE_p/V, $i_{backward}/i_{forward}$: **B**, 0.479, 0.101, 0.92; **C**, −0.742, 0.140, 0.83. Magnetic (293 K): χ_g, 5.76×10^{-6} esu; χ_{mol}(corr) 6.30×10^{-3} esu·mol^{-1}; μ_{eff} 3.85 μ_B.

Reaction between $Ru_2(ap)_4Cl$ and Excess LiC≡CC≡CSiMe$_3$. To a 20 mL THF solution containing 1.0 mmol of $Me_3SiC{\equiv}CC{\equiv}CSiMe_3$ was added 0.63 mL of BuLi (1.6 M in hexanes) at −80 °C. The mixture was slowly warmed to room temperature and stirred for an hour to yield an off-white suspension. The suspension was transferred to a flask containing a THF solution (20 mL) of $Ru_2(ap)_4Cl$ (0.184 g, 0.20 mmol). The solution color changed from dark green to reddish brown immediately, and the reaction mixture was stirred for an hour. Two different workup procedures were invoked at this point: (i) removal of THF in vacuo to yield a reddish brown residue; (ii) stirring the mixture in air for 30 min to yield a bluish green solution, followed by solvent removal. In both cases the residues were loaded on a silica gel column deactivated by 10% Et_3N in hexanes and eluted with ethyl acetate−hexanes (1:10, v/v). Yields from workup (i): **1**, 140 mg (69% based on Ru); **2**, 50 mg (22% based on Ru). Yields from workup (ii): **1**, 40 mg (19% based on Ru); **2**, 157 mg (70% based on Ru).

Data for 2: R_f 0.69 (Et_3N/ethyl acetate/hexanes, 1/1/10, v/v). MS-FAB (*m/e*, based on ^{101}Ru): 1121 [M^+]. Anal. for $C_{62}H_{62}N_8O_2Si_2Ru_2$ (**2**·EtOAc), found (calcd): C, 61.6 (60.7); H, 5.17 (5.30);

N, 9.26 (9.15). ^{1}H NMR($CDCl_3$): 9.08 (q, 4H, aromatic), 7.15 (m, 4H, aromatic), 7.04 (m, 12H, aromatic), 6.46 (m, 8H, aromatic), 5.74 (s, 8H, aromatic), 0.32 (s, 9H, $Si(CH_3)_3$), 0.18 (s, 9H, $Si(CH_3)_3$). ^{13}C NMR ($C\equiv C$, all singlet): 113.6, 109.2, 89.5, 89.3, 80.1, 79.6, 68.3, and 65.1. UV−vis, λ_{max} (nm, ϵ (M^{-1} cm^{-1})): 1046 (4810), 673 (8500), 490 (6500). IR, $\nu(C\equiv C)/cm^{-1}$: 2109(s), 2160(w). Electrochemical, $E_{1/2}$/V, ΔE_p/V, $i_{backward}/i_{forward}$: **A**, 0.896, 0.128, 0.70; **B**, −0.293, 0.105, 1.04; **C**, −1.382, 0.110, 0.74.

Reaction between $Ru_2(ap)_4Cl$ and Excess $LiC\equiv CSiMe_3$. To a 15 mL THF solution containing 5.0 mmol of $HC\equiv CSiMe_3$ was added 3.2 mL of *n*-BuLi (1.6 M in hexanes) at about −80 °C. The mixture was gradually warmed to room temperature to yield a colorless clear solution, which was added to a THF (50 mL) solution of $Ru_2(ap)_4Cl$ (0.48 g, 0.53 mmol). After the mixture was stirred under argon for 3 h, the solvent was removed on a rotovap. The residue was washed with copious amounts of warm MeOH to yield a fine green powder, which was identified as pure $Ru_2(ap)_4(C\equiv CSiMe_3)$ by TLC analysis against an authentic sample.[10] Yield: 0.47 g (91% based on Ru).

X-ray Data Collection, Processing, and Structure Analysis and Refinement. Single crystals were grown via slow cooling of saturated hexanes/ethyl acetate (**1**) and hexanes/CH_2Cl_2 (**2**) solutions. The X-ray intensity data were measured at 300 K on a Bruker SMART1000 CCD-based X-ray diffractometer system using Mo Kα (λ = 0.71073 Å). Crystals used for X-ray crystallographic analysis were cemented onto a quartz fiber with epoxy glue. Data were measured using omega scans of 0.3° per frame such that a hemisphere (1271 frames) was collected. No decay was indicated for either data set by the re-collection of the first 50 frames at the end of each data collection. The frames were integrated with the Bruker SAINT software package using a narrow-frame integration algorithm,[21] which also corrects for the Lorentz and polarization effects. Absorption corrections were applied using SADABS supplied by George Sheldrick.

The structures were solved and refined using the Bruker SHELXTL (Version 5.1) software package[22−24] in the space groups $P\bar{1}$ and $P2/c$ for crystals **1** and **2**, respectively. Positions of all non-hydrogen atoms of diruthenium moieties were revealed by direct methods. In both cases, the asymmetric unit contains one diruthenium molecule. An ethyl acetate molecule was located in the asymmetric unit of **1** and refined with distance constraints. The methyl carbon atoms of the $SiMe_3$ groups in the structures of both **1** and **2** are disordered over two positions and were refined with occupancy and distance constraints. With all non-hydrogen atoms being anisotropic and all hydrogen atoms in calculated position and riding mode the structure was refined to convergence by least-squares method on F^2, SHELXL-93, incorporated in SHELXTL.PC V 5.03. Relevant information on the data collection and the figures of merit of final refinement are listed in Table 3.

Table 3. Crystal Data for Compounds $1\cdot C_4H_8O_2$ and 2

	$\mathbf{1}\cdot C_4H_8O_2$	**2**
formula	$C_{55}H_{53}N_8O_2SiRu_2$	$C_{58}H_{54}N_8Si_2Ru_2$
fw	1088.3	1121.41
space group	$P\bar{1}$ (No. 2)	$P2/c$ (No. 13)
a, Å	10.251(2)	19.811(2)
b, Å	14.049(2)	11.864(1)
c, Å	18.963(3)	23.391(2)
α, deg	74.413(3)	90
β, deg	76.391(3)	90.717(2)
γ, deg	83.074(4)	90
volume, Å^3	2551.8(8)	5497(1)
Z	2	4
ρ_{calc}, g cm^{-3}	1.416	1.355
μ, mm^{-1}	0.664	0.637
λ(Mo Kα), Å	0.71073	0.71073
T, °C	27(2)	27(2)
no. of reflns collected	13 204	22 917
no. of ind reflns	8789 [R(int) = 0.0500]	7194 [R(int) = 0.0789]
final R indices ($I > 2\sigma(I)$)	R1 = 0.0613, wR2 = 0.1312	R1 = 0.0650, wR2 = 0.1582

Acknowledgment. We thank the University of Miami for providing support for this work (start-up fund, general research award, and the funding for the CCD-diffractometer).

Supporting Information Available: Tables of all atomic positional and equivalent isotropic displacement parameters, anisotropic displacement parameters, all bond distances and bond angles, and torsion angles of compounds **1** and **2**. This material is available free of charge via the Internet at http://pubs.acs.org.

OM001064L

---

[21] *SAINT V 6.035 Software for the CCD Detector System*; Bruker-AXS Inc., 1999.

[22] Sheldrick, G. M. *SHELXS-90, Program for the Solution of Crystal Structures*; University of Göttigen: Germany, 1990.

[23] Sheldrick, G. M. *SHELXL-93, Program for the Refinement of Crystal Structures*; University of Göttigen: Germany, 1993.

[24] *SHELXTL 5.03 (WINDOW-NT Version), Program Library for Structure Solution and Molecular Graphics*; Bruker-AXS Inc., 1998.